A CONVEX ANALYSIS BASED MINIMUM-VOLUME ENCLOSING SIMPLEX ALGORITHM FOR HYPERSPECTRAL UNMIXING

*Tsung-Han Chan†, Chong-Yung Chi†, Yu-Min Huang† and Wing-Kin Ma†**

†Inst. Commun. Eng., National Tsinghua Univ. Hsinchu, Taiwan
E-mail: cychi@ee.nthu.edu.tw

*Dept. Electronic Eng., Chinese Univ. Hong Kong Shatin, N.T., Hong Kong
E-mail: wkma@ieee.org

ABSTRACT

Hyperspectral unmixing aims at identifying the hidden spectral signatures (or endmembers) and their corresponding proportions (or abundances) from an observed hyperspectral scene. Many existing approaches to hyperspectral unmixing rely on the pure-pixel assumption, which may be violated for highly mixed data. A heuristic unmixing criterion without requiring the pure-pixel assumption has been reported by Craig: The endmember estimates are determined by the vertices of a minimum-volume simplex enclosing all the observed pixels. In this paper, using convex analysis, we show that the hyperspectral unmixing by Craig's criterion can be formulated as an optimization problem of finding a minimum-volume enclosing simplex (MVES). An algorithm that cyclically solves the MVES problem via linear programs (LPs) is also proposed. Some Monte Carlo simulations are provided to demonstrate the efficacy of the proposed MVES algorithm.

Index Terms— Convex analysis, Hyperspectral unmixing, Minimum-volume enclosing simplex, Linear programming

1. INTRODUCTION

Hyperspectral imaging has emerged as an important technique in Earth remote sensing for a wide range of applications such as terrain classification, agricultural monitoring, environmental monitoring, and military surveillance [1]. In hyperspectral imagery, each observed pixel represents a mixture of more than one distinct substances due to high spectral resolution or low spatial resolution of the airborne or spaceborne sensor used. The procedure to decompose the measured spectrum of an observed pixel into a collection of constituent spectra (or endmembers) and their corresponding proportions (or abundance fractions), or simply *hyperspectral unmixing* [2–6], is essential in identifying individual materials from a hyperspectral scene.

A number of hyperspectral unmixing algorithms adopt the assumption of existence of pure pixels (i.e., pixels that are fully contributed from a single endmember) in the observed data set. Simply speaking, those algorithms, such as PPI [2], N-FINDR [3] and VCA [4], try to search for the purest observed pixels of the data set as the endmember estimates. However, for the case of highly mixed data, the pure-pixel assumption may be violated. Hence, algorithms that do not require the pure-pixel assumption, such as alternating projected subgradients (APS) [5] and minimum volume transform (MVT) [6], would be appropriate for analysis of highly mixed data. APS solves a least squares problem with a regularization parameter that controls the abundance differences between each target and its neighbors. Furthermore, Craig [6] reported a heuristic unmixing criterion without requiring the pure-pixel assumption, that the endmember estimates are determined by the vertices of the minimum-volume simplex enclosing all the observed pixels. To find such a simplex, Craig suggested a method (i.e., MVT) that begins with a simplex of large volume and then literally moves the simplex faces in toward the data cloud.

In this paper, we propose a convex analysis based algorithm, called minimum-volume enclosing simplex (MVES) algorithm, for hyperspectral unmixing without involving pure pixels. The endeavor of employing convex analysis is motivated by the observation that some concepts, such as affine hull and convex hull, are naturally a good match to the analysis of the hyperspectral unmixing problem [7]. We first perform dimension reduction of observed pixels through affine set fitting [8], and then employ Craig's unmixing criterion [6] to formulate the hyperspectral unmixing as an MVES optimization problem that finds a simplex by minimizing the simplex volume subject to the constraint that all the dimension-reduced pixels are enclosed by the simplex. The MVES algorithm we propose is based on a cyclic minimization procedure, in which a sequence of linear programs (LPs) are solved. By computer simulations, we demonstrate that the proposed MVES algorithm is superior in performance over some existing benchmark methods.

2. SYSTEM MODEL

Consider an $M \times N$ linear spectral mixing model [1]

$$\mathbf{x}[n] = \mathbf{A}\mathbf{s}[n] = \sum_{i=1}^{N} s_i[n]\mathbf{a}_i, \qquad n = 1, \ldots, L \tag{1}$$

where $\mathbf{x}[n] = [\, x_1[n], \ldots, x_M[n] \,]^T$ is the nth observed pixel vector comprising M spectral bands, $\mathbf{A} = [\, \mathbf{a}_1, \ldots, \mathbf{a}_N \,] \in \mathbb{R}^{M \times N}$ denotes the signature matrix whose ith column vector $\mathbf{a}_i$ is the ith endmember signature, $\mathbf{s}[n] = [\, s_1[n], \ldots, s_N[n] \,]^T \in \mathbb{R}^N$ is an abundance vector comprising N fractional abundances, and L is the total number of observed pixel vectors.

The MVES algorithm to be presented is based on the following general assumptions [1]:

(A1) For all $i = 1, \ldots, N$ and $n = 1, \ldots, L$, $s_i[n] \geq 0$.

(A2) For all $n = 1, \ldots, L$, $\sum_{i=1}^{N} s_i[n] = 1$.

(A3) $\min\{L, M\} \geq N$ and $\mathbf{A}$ is of full column rank.

Assumption (A1) is true in hyperspectral imaging because intensities of all the abundance vectors must be non-negative. Assump-

This work was supported by the National Science Council (R.O.C.) under Grants NSC 96-2628-E-007-003-MY3, and by a General Research Fund of Hong Kong Research Grant Council.

tion (A2) holds true because the fractional abundances are the proportional distribution of all the endmembers in every observed pixel. Assumption (A3) is usually valid in cases where the hyperspectral scene of interest [1] involves a large number of image pixels and spectral bands but only a small number of endmembers.

3. SOME BASIC CONCEPTS OF CONVEX ANALYSIS

We review two convex analysis concepts, namely affine hull and convex hull [9], which will be prevalently used in the ensuing development. Given a set of vectors $\{\mathbf{a}_1,\ldots,\mathbf{a}_N\} \subset \mathbb{R}^M$ (a set of real M-vectors), the *affine hull* of $\{\mathbf{a}_1,\ldots,\mathbf{a}_N\}$ is defined as

$$\text{aff}\{\mathbf{a}_1,\ldots,\mathbf{a}_N\} = \left\{\mathbf{x} = \sum_{i=1}^N \theta_i \mathbf{a}_i \;\middle|\; \mathbf{1}^T\boldsymbol{\theta} = 1,\ \boldsymbol{\theta} \in \mathbb{R}^N\right\}, \quad (2)$$

where $\boldsymbol{\theta} = [\ \theta_1,\ldots,\theta_N\ ]^T$ and $\mathbf{1}$ is an all-one vector of proper dimension. An affine hull is an affine set, and therefore can always be represented by

$$\text{aff}\{\mathbf{a}_1,\ldots,\mathbf{a}_N\} = \left\{\mathbf{x} = \mathbf{C}\boldsymbol{\alpha} + \mathbf{d} \;\middle|\; \boldsymbol{\alpha} \in \mathbb{R}^P\right\} \triangleq \mathcal{A}(\mathbf{C},\mathbf{d}), \quad (3)$$

where $\mathcal{A}(\cdot,\cdot)$ is an affine set parameterized by some (non-unique) full column rank $\mathbf{C} \in \mathbb{R}^{M\times P}$ and $\mathbf{d} \in \mathbb{R}^M$. Here, P is the affine dimension which must be no more than $N-1$. If $\{\mathbf{a}_1,\ldots,\mathbf{a}_N\}$ is affinely independent (which means that $\{\mathbf{a}_1-\mathbf{a}_N,\ldots,\mathbf{a}_{N-1}-\mathbf{a}_N\}$ is linearly independent), then $P = N-1$.

Given a set of vectors $\{\mathbf{a}_1,\ldots,\mathbf{a}_N\} \subset \mathbb{R}^M$, the *convex hull* of $\{\mathbf{a}_1,\ldots,\mathbf{a}_N\}$ is defined as

$$\text{conv}\{\mathbf{a}_1,\ldots,\mathbf{a}_N\} = \left\{\mathbf{x} = \sum_{i=1}^N \theta_i \mathbf{a}_i \;\middle|\; \mathbf{1}^T\boldsymbol{\theta} = 1,\ \boldsymbol{\theta} \succeq \mathbf{0}\right\}, \quad (4)$$

where $\succeq$ stands for component-wise inequality, and $\mathbf{0}$ is an all-zero vector of proper dimension. An idea closely related to convex hull is *simplex*: A convex hull $\text{conv}\{\mathbf{a}_1,\ldots,\mathbf{a}_N\}$ is called a simplex if $\{\mathbf{a}_1,\ldots,\mathbf{a}_N\} \subset \mathbb{R}^{N-1}$ and $\mathbf{a}_1,\ldots,\mathbf{a}_N$ are affinely independent.

4. MINIMUM-VOLUME ENCLOSING SIMPLEX ALGORITHM

Now, let us introduce the MVES algorithm in this section. Under (A2) and a consequence of (A3) that $\mathbf{a}_1,\ldots,\mathbf{a}_N$ are linearly independent, one can easily infer from (1) that

$$\mathbf{x}[n] \in \text{aff}\{\mathbf{a}_1,\ldots,\mathbf{a}_N\} = \mathcal{A}(\mathbf{C},\mathbf{d}),\ \forall\, n \quad (5)$$

for some $(\mathbf{C},\mathbf{d}) \in \mathbb{R}^{M\times(N-1)} \times \mathbb{R}^M$ and $\text{rank}(\mathbf{C}) = N-1$. Thus, it is possible to recover the affine hull of $\mathbf{a}_1,\ldots,\mathbf{a}_N$ from the given observed pixels $\mathbf{x}[1],\ldots,\mathbf{x}[L]$, as stated in the following lemma:

Lemma 1. (Endmember affine set construction [8]) *Under* (A2) *and* (A3)*, the observed pixel affine hull is identical to the endmember affine hull:*

$$\mathcal{A}(\mathbf{C},\mathbf{d}) = \text{aff}\{\mathbf{x}[1],\ldots,\mathbf{x}[L]\}. \quad (6)$$

Moreover, $(\mathbf{C},\mathbf{d})$ *can be obtained from* $\{\mathbf{x}[1],\ldots,\mathbf{x}[L]\}$ *by the following closed-form solution*

$$\mathbf{d} = \frac{1}{L}\sum_{n=1}^L \mathbf{x}[n], \quad (7)$$

$$\mathbf{C} = [\ \boldsymbol{q}_1(\mathbf{U}\mathbf{U}^T), \boldsymbol{q}_2(\mathbf{U}\mathbf{U}^T),\ldots,\boldsymbol{q}_{N-1}(\mathbf{U}\mathbf{U}^T)\ ], \quad (8)$$

where $\mathbf{U} = [\ \mathbf{x}[1]-\mathbf{d},\ldots,\mathbf{x}[L]-\mathbf{d}\ ] \in \mathbb{R}^{M\times L}$*, and* $\boldsymbol{q}_i(\mathbf{R})$ *denotes the eigenvector associated with the* i*th principal eigenvalue of* $\mathbf{R}$*.*

Since $\mathbf{x}[n] \in \mathcal{A}(\mathbf{C},\mathbf{d})$, we can write its affine representation as

$$\mathbf{x}[n] = \mathbf{C}\,\tilde{\mathbf{x}}[n] + \mathbf{d}, \quad (9)$$

where $\tilde{\mathbf{x}}[n]$ is the inverse image of $\mathbf{x}[n]$ under (9), i.e.,

$$\tilde{\mathbf{x}}[n] = \mathbf{C}^\dagger(\mathbf{x}[n]-\mathbf{d}) \in \mathbb{R}^{N-1}, \quad (10)$$

where $\mathbf{C}^\dagger = (\mathbf{C}^T\mathbf{C})^{-1}\mathbf{C}^T$. The affinely transformed data $\tilde{\mathbf{x}}[n]$ for all n can be regarded as the dimension-reduced pixels. Substituting (1) into (10) yields

$$\tilde{\mathbf{x}}[n] = \sum_{j=1}^N s_j[n]\mathbf{C}^\dagger\mathbf{a}_j - \mathbf{C}^\dagger\mathbf{d}. \quad (11)$$

Since $\sum_{j=1}^N s_j[n] = 1$ [(A2)], the $\tilde{\mathbf{x}}[n]$ can be expressed as

$$\tilde{\mathbf{x}}[n] = \sum_{j=1}^N s_j[n](\mathbf{C}^\dagger\mathbf{a}_j - \mathbf{C}^\dagger\mathbf{d}) = \sum_{j=1}^N s_j[n]\boldsymbol{\alpha}_j, \quad (12)$$

where

$$\boldsymbol{\alpha}_j = \mathbf{C}^\dagger(\mathbf{a}_j - \mathbf{d}) \in \mathbb{R}^{N-1} \quad (13)$$

is the jth dimension-reduced endmember. The formulation given by (12) not only reduces the computational complexity of the subsequent processing steps, but also stimulates us to apply the simplex geometry concept to the dimension-reduced pixels $\tilde{\mathbf{x}}[1],\ldots,\tilde{\mathbf{x}}[L]$, as stated in the following lemma.

Lemma 2. (Simplex geometry) *Under (A1), (A2) and (A3),*

$$\tilde{\mathbf{x}}[n] \in \text{conv}\{\boldsymbol{\alpha}_1,\ldots,\boldsymbol{\alpha}_N\} \subset \mathbb{R}^{N-1},\ \forall n \quad (14)$$

and $\text{conv}\{\boldsymbol{\alpha}_1,\ldots,\boldsymbol{\alpha}_N\}$ *is a simplex.*

It is easy to see from (A1) and (12) that (14) is true, and the proof of $\text{conv}\{\boldsymbol{\alpha}_1,\ldots,\boldsymbol{\alpha}_N\}$ being a simplex is done by showing that $\boldsymbol{\alpha}_1,\ldots,\boldsymbol{\alpha}_N$ are affinely independent. The details are omitted here due to space limit. Lemma 2 implies that all the dimension-reduced pixels $\tilde{\mathbf{x}}[1],\ldots,\tilde{\mathbf{x}}[L]$ must be inside the simplex constructed by the dimension-reduced endmembers $\boldsymbol{\alpha}_i$ for $i = 1,...,N$. However, there exist an infinite number of solutions of $\boldsymbol{\alpha}_1,\ldots,\boldsymbol{\alpha}_N$ for which $\tilde{\mathbf{x}}[n] \in \text{conv}\{\boldsymbol{\alpha}_1,\ldots,\boldsymbol{\alpha}_N\}$ is satisfied for all n. We therefore use Craig's unmixing criterion [6] to estimate $\boldsymbol{\alpha}_1,\ldots,\boldsymbol{\alpha}_N$ by finding a simplex $\text{conv}\{\boldsymbol{\alpha}_1,\ldots,\boldsymbol{\alpha}_N\}$ that has the minimum volume and encloses all the $\tilde{\mathbf{x}}[n]$. The problem of finding an MVES can be formulated as an optimization problem as follows:

$$\boxed{\begin{array}{ll}\min\limits_{\boldsymbol{\beta}_1,\ldots,\boldsymbol{\beta}_N} & V(\boldsymbol{\beta}_1,\ldots,\boldsymbol{\beta}_N) \\ \text{s.t.} & \tilde{\mathbf{x}}[n] \in \text{conv}\{\boldsymbol{\beta}_1,\ldots,\boldsymbol{\beta}_N\},\ \forall\, n,\end{array}} \quad (15)$$

where $V(\boldsymbol{\beta}_1,\ldots,\boldsymbol{\beta}_N)$ is the volume of the simplex $\text{conv}\{\boldsymbol{\beta}_1,\ldots,\boldsymbol{\beta}_N\}$ [10], given by

$$V(\boldsymbol{\beta}_1,\ldots,\boldsymbol{\beta}_N) = |\det(\mathbf{B})|/(N-1)! \quad (16)$$

where

$$\mathbf{B} = [\ \boldsymbol{\beta}_1-\boldsymbol{\beta}_N,\ldots,\boldsymbol{\beta}_{N-1}-\boldsymbol{\beta}_N\ ] \in \mathbb{R}^{(N-1)\times(N-1)}. \quad (17)$$

Figure 1 illustrates what the MVES problem tries to solve geometrically for $N = 3$, where the solid-line triangle is supposed to be the optimal simplex whose area is smaller than that of any other triangles enclosing all the dimension-reduced data, e.g., the dashed-line triangle.

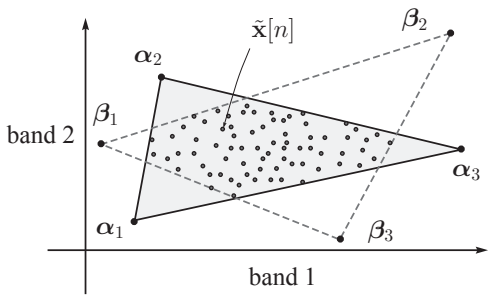

Fig. 1. Scatter plot of two-dimensional dimension-reduced pixels illustrating the MVES problem for hyperspectral unmixing.

Next, we turn our attention to solving the MVES problem (15). We first reformulate problem (15) into a determinant maximization problem that follows.

Any $\tilde{\mathbf{x}}[n] \in \text{conv}\{\boldsymbol{\beta}_1, \ldots, \boldsymbol{\beta}_N\}$ can be represented by

$$\tilde{\mathbf{x}}[n] = \boldsymbol{\beta}_N + \mathbf{B}\mathbf{s}'[n], \tag{18}$$

where $\mathbf{s}'[n] = [\ s_1[n], \ldots, s_{N-1}[n]\ ]^T \succeq \mathbf{0}$ and $s_N[n] = 1 - \mathbf{1}^T\mathbf{s}'[n] \geq 0$. Therefore, problem (15) is then formulated as

$$\begin{array}{ll} \min\limits_{\substack{\mathbf{B},\, \boldsymbol{\beta}_N,\\ \mathbf{s}'[1],\ldots,\mathbf{s}'[L]}} & |\det(\mathbf{B})| \\ \text{s.t.} & \mathbf{s}'[n] \succeq \mathbf{0},\ \mathbf{1}_{N-1}^T\mathbf{s}'[n] \leq 1, \\ & \tilde{\mathbf{x}}[n] = \boldsymbol{\beta}_N + \mathbf{B}\mathbf{s}'[n],\ \forall\, n = 1, \ldots, L. \end{array} \tag{19}$$

Problem (19) is a hard problem because of the highly nonlinear, nonconvex nature of the objective function $|\det(\mathbf{B})|$, and nonlinear equality constraints.

To describe the proposed MVES algorithm, we consider the following problem reformulation that will help alleviate the difficulty in solving (19). Let

$$\mathbf{H} = \mathbf{B}^{-1} \in \mathbb{R}^{(N-1)\times(N-1)}, \tag{20a}$$

$$\mathbf{g} = \mathbf{B}^{-1}\boldsymbol{\beta}_N \in \mathbb{R}^{N-1}. \tag{20b}$$

Then $\mathbf{s}'[n]$ can be represented as

$$\mathbf{s}'[n] = \mathbf{B}^{-1}(\tilde{\mathbf{x}}[n] - \boldsymbol{\beta}_N) = \mathbf{H}\tilde{\mathbf{x}}[n] - \mathbf{g}. \tag{21}$$

Substituting (20) and (21) into (19) yields

$$\begin{array}{ll} \max\limits_{\mathbf{H},\, \mathbf{g}} & |\det(\mathbf{H})| \\ \text{s.t.} & \mathbf{H}\tilde{\mathbf{x}}[n] - \mathbf{g} \succeq \mathbf{0},\ \mathbf{1}^T(\mathbf{H}\tilde{\mathbf{x}}[n] - \mathbf{g}) \leq 1,\ \forall\, n, \end{array} \tag{22}$$

in which all constraints become linear.

We propose to apply a cyclic maximization procedure on (22). The idea is motivated by the cofactor expansion of $\det(\mathbf{H})$ as follows

$$\det(\mathbf{H}) = \sum_{j=1}^{N-1}(-1)^{i+j}h_{ij}\det(\boldsymbol{\mathcal{H}}_{ij}), \tag{23}$$

for any $i = 1, \ldots, N-1$, where h_{ij} is the (i,j)th entry of $\mathbf{H}$, and $\boldsymbol{\mathcal{H}}_{ij} \in \mathbb{R}^{(N-2)\times(N-2)}$ is a submatrix of $\mathbf{H}$ with the ith row and jth column removed [10]. Note that with a fixed $\boldsymbol{\mathcal{H}}_{ij}$, $\det(\mathbf{H})$ is a linear function with respect to h_{ij}. Let us consider updating one row vector of $\mathbf{H}$ and one entry of $\mathbf{g}$ while fixing the other rows of $\mathbf{H}$ and the other entries of $\mathbf{g}$. Let $\mathbf{h}_i^T$ denote the ith row vector of $\mathbf{H}$, and g_i denote the ith entry of $\mathbf{g}$. The partial maximization of (22) with respect to $\mathbf{h}_i$ and g_i is given by

$$\begin{array}{ll} \max\limits_{\mathbf{h}_i^T,\, g_i} & \Big|\sum\limits_{j=1}^{N-1}(-1)^{i+j}h_{ij}\det(\boldsymbol{\mathcal{H}}_{ij})\Big| \\ \text{s.t.} & 0 \leq \mathbf{h}_i^T\tilde{\mathbf{x}}[n] - g_i \leq 1 - \sum\limits_{j\neq i}(\mathbf{h}_j^T\tilde{\mathbf{x}}[n] - g_j),\ \forall\, n. \end{array} \tag{24}$$

Note that the objective function in (24) is still nonconvex. However, the partial maximization problem in (24) can be solved in a globally optimal manner by breaking it into two LPs:

$$\begin{array}{ll} p^\star = \max\limits_{\mathbf{h}_i^T,\, g_i} & \sum\limits_{j=1}^{N-1}(-1)^{i+j}h_{ij}\det(\boldsymbol{\mathcal{H}}_{ij}) \\ \text{s.t.} & 0 \leq \mathbf{h}_i^T\tilde{\mathbf{x}}[n] - g_i \leq 1 - \sum\limits_{j\neq i}(\mathbf{h}_j^T\tilde{\mathbf{x}}[n] - g_j),\ \forall\, n. \end{array} \tag{25}$$

$$\begin{array}{ll} q^\star = \min\limits_{\mathbf{h}_i^T,\, g_i} & \sum\limits_{j=1}^{N-1}(-1)^{i+j}h_{ij}\det(\boldsymbol{\mathcal{H}}_{ij}) \\ \text{s.t.} & 0 \leq \mathbf{h}_i^T\tilde{\mathbf{x}}[n] - g_i \leq 1 - \sum\limits_{j\neq i}(\mathbf{h}_j^T\tilde{\mathbf{x}}[n] - g_j),\ \forall\, n. \end{array} \tag{26}$$

The optimal solution of (24), denoted by $((\mathbf{h}_i^T)^\star, g_i^\star)$, is chosen to be the optimal solution of (25) if $|p^\star| > |q^\star|$, and the optimal solution of (26) if $|q^\star| > |p^\star|$. This row-wise minimization is conducted cyclically (i.e., $i := (i \text{ modulo } (N-1)) + 1$ at each iteration) until some stopping rule is satisfied.

Suppose that a solution $(\mathbf{H}^\star, \mathbf{g}^\star)$ is obtained by the cyclic maximization of (22). By (17) and (20) where $\boldsymbol{\beta}_i$, $\mathbf{H}$ and $\mathbf{g}$ are replaced by $\widehat{\boldsymbol{\alpha}}_i$, $\mathbf{H}^\star$ and $\mathbf{g}^\star$, respectively, the dimension-reduced endmember estimates, denoted $\widehat{\boldsymbol{\alpha}}_i$ for all i, are given by

$$\widehat{\boldsymbol{\alpha}}_N = (\mathbf{H}^\star)^{-1}\mathbf{g}^\star, \tag{27}$$

$$[\widehat{\boldsymbol{\alpha}}_1, ..., \widehat{\boldsymbol{\alpha}}_{N-1}] = \widehat{\boldsymbol{\alpha}}_N\mathbf{1}^T + (\mathbf{H}^\star)^{-1}. \tag{28}$$

The endmember signatures can then be recovered by (13), i.e., $\widehat{\mathbf{a}}_i = \mathbf{C}\widehat{\boldsymbol{\alpha}}_i + \mathbf{d}$ for $i = 1, \ldots, N$. Furthermore, from (21), the abundance vectors can be estimated as

$$\begin{aligned} \widehat{\mathbf{s}}[n] &= [\ \mathbf{s}'[n]^T \quad 1 - \mathbf{1}^T\mathbf{s}'[n]\ ]^T, \\ &= [\ (\mathbf{H}^\star\tilde{\mathbf{x}}[n] - \mathbf{g}^\star)^T \quad 1 - \mathbf{1}^T(\mathbf{H}^\star\tilde{\mathbf{x}}[n] - \mathbf{g}^\star)\ ]^T, \forall\, n. \end{aligned} \tag{29}$$

To initialize the proposed MVES algorithm, a feasible $(\mathbf{H}, \mathbf{g})$ for solving problem (24) is needed. We can find one by solving the following feasibility problem:

$$\begin{array}{ll} \text{find} & (\mathbf{H}, \mathbf{g}) \\ \text{s.t.} & \mathbf{H}\tilde{\mathbf{x}}[n] - \mathbf{g} \succeq \mathbf{0},\ \mathbf{1}^T(\mathbf{H}\tilde{\mathbf{x}}[n] - \mathbf{g}) \leq 1,\ \forall\, n, \end{array} \tag{30}$$

which can also be implemented by LP.

5. SIMULATIONS AND CONCLUSION

We performed 100 Monte Carlo runs with the proposed MVES algorithm and four existing unmixing algorithms, PPI [2], N-FINDR [3], VCA [4] and APS [5] for performance comparison. Since PPI, N-FINDR, and VCA can only obtain endmember estimates, the fully constrained least squares (FCLS) [11] was used to find the associated abundances in the simulations. Let $\hat{\mathbf{a}}_1, \ldots, \hat{\mathbf{a}}_N$ denote

the estimated endmembers, and let $\boldsymbol{s}_1, \ldots, \boldsymbol{s}_N$ and $\hat{\boldsymbol{s}}_1, \ldots, \hat{\boldsymbol{s}}_N$ denote the true and estimated abundances, respectively, where $\boldsymbol{s}_i = [\ s_i[1], \ldots, s_i[L]\ ]^T \in \mathbb{R}^L$ and $\hat{\boldsymbol{s}}_i = [\ \hat{s}_i[1], \ldots, \hat{s}_i[L]\ ]^T \in \mathbb{R}^L$. The endmember estimation performance was measured by the following root-mean-square (rms) spectral angle [4]

$$\phi_{en} = \min_{\boldsymbol{\pi} \in \Pi_N} \sqrt{\frac{1}{N} \sum_{i=1}^{N} \left[\arccos \left(\frac{\mathbf{a}_i^T \hat{\mathbf{a}}_{\pi_i}}{\|\mathbf{a}_i\| \|\hat{\mathbf{a}}_{\pi_i}\|} \right) \right]^2} \qquad (31)$$

where $\boldsymbol{\pi} = (\pi_1, \ldots, \pi_N)$, and $\Pi_N = \{\boldsymbol{\pi} \in \mathbb{R}^N \mid \pi_i \in \{1, 2, \ldots, N\},\ \pi_i \neq \pi_j \text{ for } i \neq j\}$ is the set of all the permutations of $\{1, 2, ..., N\}$. Similarly, the performance measure for the estimated abundances is

$$\phi_{ab} = \min_{\boldsymbol{\pi} \in \Pi_N} \sqrt{\frac{1}{N} \sum_{i=1}^{N} \left[\arccos \left(\frac{\boldsymbol{s}_i^T \hat{\boldsymbol{s}}_{\pi_i}}{\|\boldsymbol{s}_i\| \|\hat{\boldsymbol{s}}_{\pi_i}\|} \right) \right]^2} \qquad (32)$$

Clearly, the smaller the values of ϕ_{en} and ϕ_{ab}, the better the performance of the unmixing algorithm.

At each Monte Carlo run six endmembers (i.e., Alunite, Buddingtonite, Calcite, Copiapite, Kaolinite, and Muscovite) with 417 bands selected from the U.S. geological survey (USGS) library [12] were used to produce 1000 observed pixels (i.e., $N = 6$, $M = 417$, $L = 1000$). The corresponding abundances $\mathbf{s}[n]$ were synthetically generated following a Dirichlet distribution $D(\mathbf{s}[n], \boldsymbol{\mu})$ with $\boldsymbol{\mu} = \frac{1}{N}\mathbf{1}$ which automatically enforces (A1) and (A2) [4].

To generate the observed data set with different purity levels, let us define a purity measure for an observed pixel $\mathbf{x}[n]$, indicating how quantitatively $\mathbf{x}[n] = \mathbf{A}\mathbf{s}[n]$ is dominated by a single endmember, as follows

$$\rho_n = \frac{\|\mathbf{s}[n]\|}{\mathbf{1}^T \mathbf{s}[n]} = \|\mathbf{s}[n]\| \qquad (33)$$

due to (A2). Note that $1/\sqrt{N} \leq \rho_n \leq 1$ and the purity of the observed pixel $\mathbf{x}[n]$ is higher for larger ρ_n. A set of L observed pixels $\mathbf{x}[n]$ with $\rho - 0.1 \leq \rho_n \leq \rho$ is called a data set with purity level of ρ (where $(0.1 + 1/\sqrt{N}) \leq \rho \leq 1$), which can be generated through the following steps.

(S1) Generate a set of $K = 10L$ observed pixels where the abundance vectors $\mathbf{s}[k]$ following a Dirichlet distribution, i.e.,

$$\Omega = \left\{ \mathbf{x}[k] = \mathbf{A}\mathbf{s}[k] \;\middle|\; \mathbf{s}[k] \sim D(\mathbf{s}[k], \boldsymbol{\mu}),\ \forall k = 1, \ldots, K \right\},$$

and calculate the corresponding purity $\rho_k = \|\mathbf{s}[k]\|$ of each $\mathbf{x}[k]$ for all k.

(S2) Construct the set of observed pixels with purity level equal to ρ by randomly picking L observed pixels from Ω while satisfying $\rho_n \in [\rho - 0.1, \rho]$, i.e.,

$$\{\mathbf{x}[n] \mid \mathbf{x}[n] \in \Omega,\ \rho_n \in [\rho - 0.1, \rho],\ \forall n = 1, \ldots, L\}.$$

Note that the generated data for $\rho = 1$ include some $\mathbf{x}[n]$ with $\rho_n \simeq 1$, i.e., highly pure pixels.

The average ϕ_{en} and ϕ_{ab} of the unmixing methods for different values of $\rho = 0.7, 0.75, \ldots, 1$ are shown in Figure 2, where all the algorithms perform better for higher purity level, except for APS. The notably superior performance of the MVES algorithm over the others can be observed for lower ρ.

In conclusion, we have presented a convex analysis based MVES algorithm for hyperspectral unmixing without involving pure pixels. The proposed method uses LPs to solve the MVES problem in a cyclic fashion. Simulation results give a good validation of the better performance of the proposed method, compared to some existing benchmark methods.

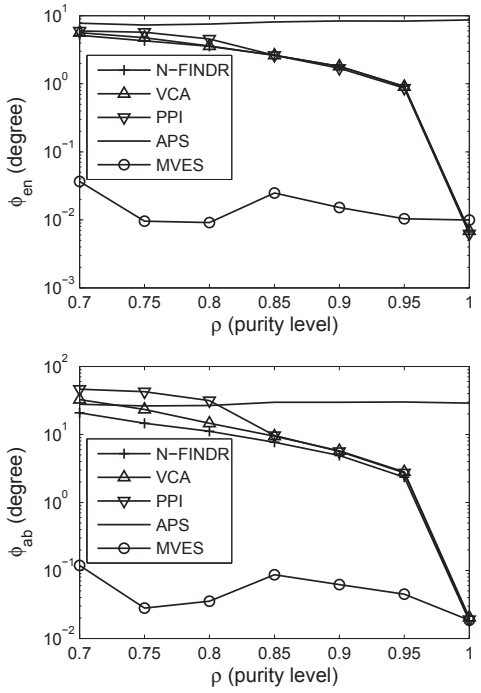

Fig. 2. Simulation results (ϕ_{en} and ϕ_{ab}) for the estimates of endmember and abundances obtained by PPI, N-FINDR, VCA, APS, and MVES algorithm.

6. REFERENCES

[1] N. Keshava and J. Mustard, "Spectral unmixing," *IEEE Signal Process. Mag.*, vol. 19, no. 1, pp. 44-57, Jan. 2002.

[2] J. W. Boardman, F. A. Kruse, and R. O. Green, "Mapping target signatures via partial unmixing of AVRIS data," in *Proc. Summ. JPL Airborne Earth Sci. Workshop*, Pasadena, CA, Dec. 9-14, 1995, pp. 23-26.

[3] M. E. Winter, "N-findr: An algorithm for fast autonomous spectral end-member determination in hyperspectral data," in *Proc. SPIE Conf. Imaging Spectrometry, Pasadena*, CA, Oct. 1999, pp. 266-275.

[4] J. M. P. Nascimento and J. M. B. Dias, "Vertex component analysis: A fast algorithm to unmix hyperspectral data," *IEEE Trans. Geosci. Remote Sens.*, vol. 43, no. 4, pp. 898-910, Apr. 2005.

[5] A. Zymnis, S.-J. Kim, J. Skaf, M. Parente, and S. Boyd, "Hyperspectral image unmixing via alternating projected subgradients," in *41st Asilomar Conference on Signals, Systems, and Computers*, Pacific Grove, CA, Nov. 4-7, 2007.

[6] M. D. Craig, "Minimum-volume transforms for remotely sensed data," *IEEE Trans. Geosci. Remote Sens.*, vol. 32, no. 3, pp. 542-552, May 1994.

[7] J. W. Boardman, "Automating spectral unmixing of AVIRIS data using convex geometry concepts," in *Proc. Summ. 4th Annu. JPL Airborne Geosci. Workshop*, Dec. 9-14, 1993, vol. 1, pp. 11-14.

[8] T.-H. Chan, W.-K. Ma, C.-Y. Chi, and Y. Wang, "A convex analysis framework for blind separation of non-negative sources," *IEEE Trans. Signal Processing*, vol. 56, no. 10, pp. 5120-5134, Oct. 2008.

[9] S. Boyd and L. Vandenberghe, *Convex Optimization*, Cambridge Univ. Press, 2004.

[10] G. Strang, *Linear Algebra and Its Applications*, CA: Thomson, 4th edition, 2006.

[11] D. Heinz and C.-I. Chang, "Fully constrained least squares linear mixture analysis for material quantification in hyperspectral imagery," *IEEE Trans. Geosci. Remote Sens.*, vol. 39, no. 3, pp. 529-545, Mar. 2001.

[12] Tech. Rep., Available online: `http://speclab.cr.usgs.gov/cuprite.html`.